Proceedings of the 3rd IASME/WSEAS Int. Conf. on HEAT TRANSFER, THERMAL ENGINEERING AND ENVIRONMENT, Corfu, Greece, August 20-22, 2005 (pp198-203)

Buoyancy-Driven Convection in a Horizontal Fluid Layer Subjected to Isothermal Cooling from Above

J.H. PARK[1], M.C. KIM[2], J.H. MOON[1], S.H. PARK[1], C.K. CHOI[1,*]
[1]School of Chemical and Biological Engineering, Seoul National University, Seoul 151-744, KOREA
[2]Department of Chemical Engineering, Cheju National University, Cheju 690-756, KOREA

Abstract: - The temporal behavior of buoyancy-driven convection in an initially quiescent, horizontal fluid layer cooled from above with a fixed surface temperature is investigated theoretically. In the present system, the conduction temperature profile develops with time and it becomes an important question to predict the onset time of thermal convection. Here the Boussinesq equation is solved numerically by using the finite volume method. The temporal growth rates of the mean temperature and its fluctuations are examined. In the present study, based on the numerical results, the characteristic times to represent the temporal behavior of thermal convection are illustrated. They are compared and discussed in comparison with existing experimental data. The new concept to decide the onset conditions of intrinsic instability is suggested here.

Key-Words: - Buoyancy-Driven Convection, Temporal Growth Rate, Intrinsic Instability, Undershoot Time, Isothermal Cooling, Fluctuation, Rayleigh Number

1 Introduction

When a horizontal fluid layer is heated from below or cooled from above, natural convection can set in due to buoyancy forces. In rapidly cooled or heated systems, nonlinear temperature profiles develop with time and the prediction of the critical time to mark the onset of convective instability becomes an important question. The related instability problem has been analyzed by using the frozen-time model [1], propagation theory [2], amplification theory [3], stochastic model [4], and maximum-Rayleigh number criterion [5]. But this problem still remains unresolved because of its inherent complexity. The first two models based on linear theory yield the characteristic times to represent the onset of a fastest growing instability. The last three models deal with the onset of manifest convection, which is usually described as the deviation of the base temperature field from its conduction solution. But it is known that the convective motion is detected before the manifestation of thermal convection. The third and fourth models are dependent upon the initial conditions at time t=0 and require the measure to ensure initiated manifest convection.

For the specific case of the system cooled from above, Spangenberg and Rowland [6] and Foster [7] conducted the related experiments with the evaporative cooling method. Foster [3], Kaviany [8], Tan and Thorpe [5], and Choi et al. [9] analyzed the related stability problems. The boundary conditions in their studies are constant-heat-flux or time-dependent temperature. Plevan and Quinn [10], Blair and Quinn [11], and Tan and Thorpe [12] adopted the gas absorption systems. When a horizontal liquid layer experiences sudden density change by gas absorption into a liquid, buoyancy- driven convection can set in. The initiated motion is similar to convection in the system cooled isothermally from above. They observed the onset of convection with schlieren photography. In this case the upper boundary usually has the free-surface condition.

In the present study, the onset of convective instability in a horizontal fluid layer subjected to isothermal cooling from above is analyzed. In this time-dependent system it is important to predict the characteristic times to represent the transient behavior of convective instability. Here the critical time to mark the onset of convective instability, t_c, is first suggested. For $t>t_c$, instability can grow until the manifest convection is observed at $t=t_D$. At $t=t_u$ the minimum Nusselt number is exhibited in the plot of the Nusselt number versus time. The previous models do not illustrate the difference among the above characteristic times. Accordingly, we will employ the finite volume method (FVM) to examine the transient behavior of convective instability and the resulting characteristic times will be discussed in comparison with available experimental data.

Proceedings of the 3rd IASME/WSEAS Int. Conf. on HEAT TRANSFER, THERMAL ENGINEERING AND ENVIRONMENT, Corfu, Greece, August 20-22, 2005 (pp198-203)

2 Governing Equation

The system considered here is a horizontal fluid layer of thickness H, as shown in Fig. 1. For $t \geq 0$, the fluid layer with an initial temperature T_i is cooled from above with a lower temperature T_u at the vertical distance Z=0. The bottom temperature is kept constant at $T=T_i$. For a high ΔT (=$T_i - T_u$), the nonlinear developing temperature profiles are formed and the buoyancy-driven convection sets in at a certain time. The governing equations of the flow and temperature fields can be expressed in dimensionless form with the Boussinesq approximation:

$$\nabla \cdot \boldsymbol{u} = 0 \tag{1}$$

$$(\partial/\partial\tau + \boldsymbol{u}\cdot\nabla)\boldsymbol{u} = -\nabla p + Pr\nabla^2\boldsymbol{u} + Pr\,Ra\theta\,\boldsymbol{k} \tag{2}$$

$$(\partial/\partial\tau + \boldsymbol{u}\cdot\nabla)\theta = \nabla^2\theta \tag{3}$$

with the boundary conditions,

$$\partial u/\partial z = \partial v/\partial z = w = \partial^2 w/\partial z^2 = 0,\ \theta = 1 \ \text{ at } \ z = 0 \quad \text{(4a, b)}$$

$$u = v = w = \partial w/\partial z = 0,\ \theta = 0 \ \text{ at } \ z = 1 \quad \text{(5a, b)}$$

where θ (=$(T-T_i)/(T_u-T_i)$), p (=$PH^2/(\rho\alpha^2)$), τ (=$\alpha t/H^2$), and $\boldsymbol{u}$ (=$\boldsymbol{i}u+\boldsymbol{j}v+\boldsymbol{k}w$) denote the dimensionless forms of the temperature T, the pressure P, the time t, and the velocity vector $\boldsymbol{U}$ (=($\alpha\boldsymbol{u}/H$)), respectively. Here α, β, g and ρ, respectively, represent the thermal diffusivity, the thermal expansion coefficient, the gravitational acceleration constant, and the fluid density at $T=T_i$. The Cartesian coordinates (x, y, z) have the scale of H, $\boldsymbol{k}$ is the vertical unit vector, and ($\boldsymbol{i}, \boldsymbol{j}$) are the horizontal ones. The important parameters describing the present system, the Prandtl number Pr and the Rayleigh number Ra, are defined as

$$Pr = \frac{\nu}{\alpha},\quad Ra = \frac{g\beta\Delta T H^3}{\alpha\nu} \tag{6}$$

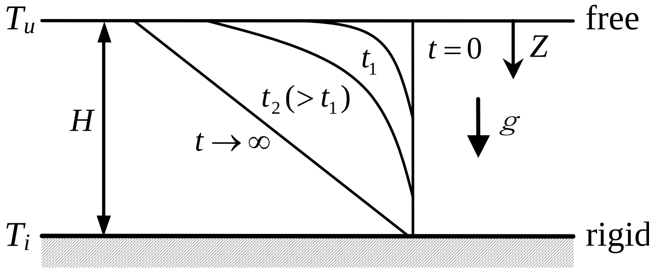

Fig. 1. Schematic diagram of the system considered

where ν is the kinematic viscosity. It is well-known that in the present system natural convection exists for $Ra \geq 1101$.

3 Onset of Convective Instability

3.1 Temporal growth rate

The velocity and temperature fields can be divided into the mean quantities and their fluctuations as follows:

$$\boldsymbol{u} = \langle\boldsymbol{u}\rangle + \boldsymbol{u}' \tag{7}$$

$$\theta = \langle\theta\rangle + \theta' \tag{8}$$

where $\langle\cdot\rangle$ and $'$ represent the horizontal mean and their fluctuations, respectively. The mean quantity is a function of τ and z, and it is known that $\langle\boldsymbol{u}\rangle$=0 for the flow in form of regular even cells.

In the present system, thermal convection sets in due to the buoyancy force and its magnitude F_B is represented by

$$F_B = \rho g\beta|T - T_i| \tag{9}$$

which is produced by temperature variations. The buoyancy forces based on the mean temperature and its fluctuations can be written as $(F_{B,0}, F_{B,1}) = (\langle\theta\rangle, \theta')\rho g\beta\Delta T$, where $F_B = F_{B,0} + F_{B,1}$. In order to examine the temporal behavior of thermal instability the following temporal growth rates are defined:

$$r_{0,\mathrm{T}} = \frac{1}{\langle\theta\rangle_{rms}}\frac{d\langle\theta\rangle_{rms}}{d\tau} \tag{10}$$

$$r_{1,\mathrm{T}} = \frac{1}{\theta'_{rms}}\frac{d\theta'_{rms}}{d\tau} \tag{11}$$

where $r_{0,\mathrm{T}}$ and $r_{1,\mathrm{T}}$ are, respectively, the temporal growth rates of the mean temperature and the temperature fluctuations. The subscript '*rms*' refers to the root-mean-square quantity, *i.e.*, $(\cdot)_{rms} = [\int_V(\cdot)^2 dV/V]^{1/2}$, where V represents the volume of the system considered. Also, we define the temporal growth rate of velocity fluctuations as follows:

$$r_{1,\mathrm{V}} = \frac{1}{\boldsymbol{u}'_{rms}}\frac{d\boldsymbol{u}'_{rms}}{d\tau} \tag{12}$$

Proceedings of the 3rd IASME/WSEAS Int. Conf. on HEAT TRANSFER, THERMAL ENGINEERING AND ENVIRONMENT, Corfu, Greece, August 20-22, 2005 (pp198-203)

where $\boldsymbol{u}'_{rms} = [\int_V |\boldsymbol{u}'|^2 dV/V]^{1/2}$.

3.2 Temporal behavior of thermal instability

In the present time-dependent problem the selection of the initial conditions is very important. According to experimental observations fluctuations are assumed to show periodic patterns as follows:

$$[\theta', \boldsymbol{u}'] \cong [A(\tau)\theta_*(z), B(\tau)\boldsymbol{u}_*(z)]\exp(iay) \quad \text{for } 0 \le \tau \le \tau_c \qquad (13)$$

where i is the imaginary unit and $a\,(=(a_x^2+a_y^2)^{1/2})$ is the dimensionless wavenumber and. Here A and B are the magnitudes of fluctuations and τ_c denotes the critical time to mark the onset of convective instability. The functions θ_* and $\boldsymbol{u}_*$ represent the normalized temperature and velocity fluctuations, respectively. For a horizontally infinite layer, only y may be used as the horizontal distance. The initial conditions at τ=0 for the two-dimensional fluctuations are constructed as $\theta'=A(0)\theta_*(z)\cos(ay)$, $v'=-B(0)((\partial w_*(z)/\partial z)/a)\sin(ay)$ and $w'=B(0)w_*(z)\cos(ay)$, where $A(0)$ and $B(0)$ are the initial magnitudes. Here it is assumed that $\theta_*(z)$ and $\boldsymbol{u}_*(z)$ would not change for $0 \le \tau \le \tau_c$. Therefore, the unique disturbance patterns are decided with the converged disturbance profiles by iterating the calculation for $0 \le \tau \le \tau_c$.

The critical condition of instrinsic instability is suggested here:

$$r_{1,\mathrm{T}} = r_{0,\mathrm{T}} \quad \text{with } r_{1,\mathrm{V}} \ge 0 \quad \text{at } \tau = \tau_c \qquad (14)$$

This means that the convective motion of a=a_c to satisfy Eq. (13) sets in at the earliest time τ_c. For $\tau < \tau_c$, fluctuations are so small in comparison with the conduction temperature field and they may be called noises. For $\tau > \tau_c$, buoyancy-driven instabilities can grow with time until they are detected at a certain time. Therefore, the system is assumed stable with $r_{1,\mathrm{T}} < r_{0,\mathrm{T}}$ but unstable with $r_{1,\mathrm{T}} > r_{0,\mathrm{T}}$.

In the present study the Nusselt number Nu with the characteristic length of H is defined as follows:

$$Nu = \int_S (-\partial\theta/\partial z)_{z=0}\, dS \Big/ S \qquad (15)$$

where S is the surface area of the top plate. With thermal convection, Nu deviates from its conduction solution and has the minimum at τ=τ_u. The undershoot time τ_u is frequently used as the characteristic time to ensure the manifestation of thermal convection.

4 Numerical Method

The governing equations and the boundary conditions (1)-(5) were solved numerically by using the FVM introduced by Patankar [13]. Here two-dimensional motion with horizontal periodicity was considered and one convection cell with the proper side-boundary conditions was chosen to describe the horizontally infinite layer. The SIMPLE algorithm was applied to solve the pressure equation and the hybrid scheme was used to formulate the discretization equations. In order to solve the present time-dependent problem the implicit method was adopted and the first-order time increment was used. The number of meshes was 42×60 and finer meshes were used near the top and bottom boundaries to guarantee the physical validity. Also, to ensure the numerical stability the time step of $\Delta\tau$=10^{-7} was used. In the present problem, the convergence was assumed when the changes of velocities and temperature were smaller than 10^{-6} at each time step.

With the proper magnitude of the initial temperature and velocity fields, $A(0)$ and $B(0)$, the present system was simulated numerically for a given Ra and Pr. The proper $A(0)$-value was found to be 10^{-3} in comparsion with available experimental data. In the present study, the numerical simulation was conducted for $Pr\to\infty$ and the τ_c- and τ_u-values were obtained.

5 Results and Discussion

The results of the numerical simulation by the FVM with $Pr\to\infty$ are reported here. Based on Eqs. (10)-(12), the stability criteria to satisfy the condition (14) are assumed to represent a fastest growing instability.

With Ra=$10^6$and $A(0)$=10^{-3}, the temporal behaviors of fluctuations are shown in Fig. 2. This $A(0)$-value was used by Choi et al. [14] and Chung et al. [15] for the case of an isothermal heating, which agrees well with the experimental data of high Rayleigh numbers in the transient Rayleigh-Bénard convection. For small τ, w'_{rms} and θ'_{rms} retain almost the same magnitudes as their initial ones. But for $2\times10^{-4} < \tau < 2\times10^{-3}$ they experience a sudden increase. The temporal growth rates given by Eqs. (10)-(12) are illustrated in Fig. 3. The instability criterion (14) yields τ_c=2.0×10^{-4} and a_c=12 for Ra=10^6. The maximum values of $r_{1,\mathrm{T}}$

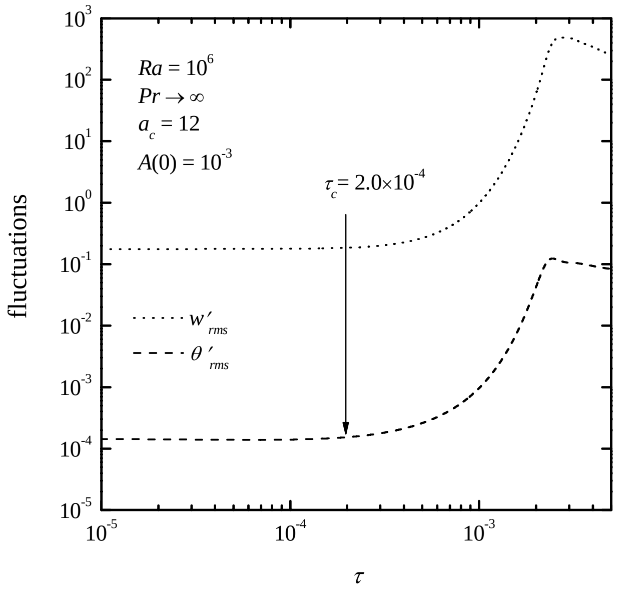

Fig. 2. Temporal behavior of fluctuations

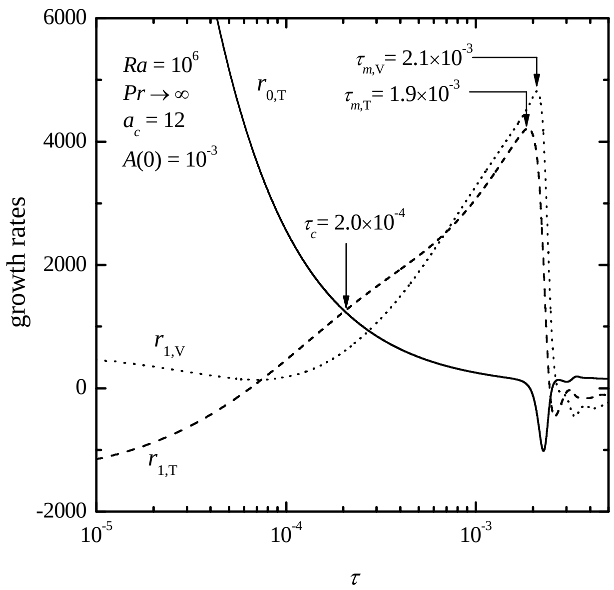

Fig. 3. Temporal growth rates for $Ra=10^6$

and $r_{1,\mathrm{V}}$ appear at $\tau=\tau_{m,\mathrm{T}}$ and $\tau=\tau_{m,\mathrm{V}}$, respectively. Here the $r_{1,\mathrm{T}}$- and $r_{1,\mathrm{V}}$-paths are the unique ones. The $r_{1,\mathrm{T}}$-path is almost independent of the initial velocity condition for $Pr\to\infty$. In the present problem of buoyancy-driven convection, convective instability occurs due to temperature variations. Therefore, $r_{1,\mathrm{T}}$ seems to play a critical role rather than $r_{1,\mathrm{V}}$.

As shown in Fig. 4, the τ_c-value is independent of the A(0)-value for $10^{-2}<A(0)<10^{-6}$ but the $\tau_{m,\mathrm{T}}$- and $\tau_{m,\mathrm{V}}$-values are dependent upon it. Therefore, it is stated that the present τ_c-value is the invariant and it represents the onset time of intrinsic instability. The developing behavior of the Nusselt number with time is illustrated in Fig. 5. The present numerical simulation yields the undershoot time $\tau_u=1.8\times10^{-3}$ with $A(0)=10^{-3}$ in the plot of Nu versus τ. The undershoot time represents the characteristic time for the manifestation of convection. The τ_u-value is also dependent upon the A(0)-value, as shown in Fig. 5. Also, it is known that $\tau_u\cong\tau_{m,\mathrm{T}}\cong\tau_{m,\mathrm{V}}$. The incipient instability at $\tau=\tau_c$ will grow with increasing τ and the convective motion will be detected at $\tau=\tau_D$. The detection time of motion is prior to the undershoot time of the Nusselt number. The detection time of convective motion may be closely connected with $r_{1,\mathrm{V}}$ and the earliest-detection time τ_D would be located between τ_c and $\tau_{m,\mathrm{V}}$. Here the relation of $\tau_c\leq\tau_D\leq\tau_{m,\mathrm{V}}$ ($\cong\tau_u$) is suggested.

Plevan and Quinn [10] and Tan and Thorpe [12] observed the onset of buoyancy-driven convection in the gas absorption system. For systems of gas absorption into aqueous carboxy methyl cellulose (CMC) solutions, the onset time of convection was reported. Their experimental data of CMC solutions agree well with the present τ_u-values with $A(0)=10^{-3}$ for $Pr\to\infty$, as shown in Fig. 6. Therefore, it is stated that the present simulation represents the actual system well. Here it is known that $\tau_u=9\tau_c$. The growth period is required from the onset of intrinsic instability to the manifestation of convection. In connection with the growth period Foster [16] suggested the amplification factor to ensure manifest convection. He commented that the onset time of manifest convection would be four times larger than the onset time of instability. Tan and Thorpe [12] suggested the onset time of convection as $\tau_o=37.0Ra^{-2/3}$, where τ_o is their critical time. This is shown in Fig. 6. Their predicted critical times are higher than experimental values. They [17] suggested the same relation when the rigid bottom surface is heated isothermally. It is not reasonable that the cases of cooling the free surface and heating the rigid surface yield the same critical times.

Blair and Quinn [11] conducted the experiment for gas aborption systems using water instead of CMC solutions. They showed that a upper free surface behaves as if it is flexible and laterally rigid because of the presence of minute traces of surface-active contaminants. Their experimental data are compared with the present numerical results in Fig. 7 and it is known that they deviate much from the numerical τ_u-values. We obtained the numerical results for the

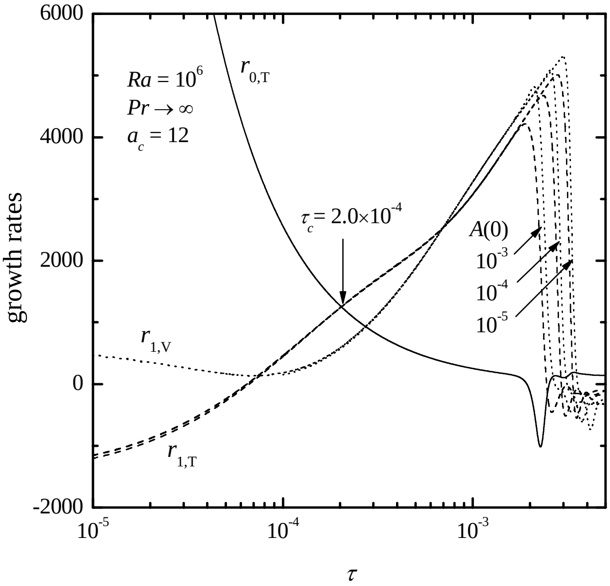

Fig. 4. Dependence of growth rates on the A(0)-value

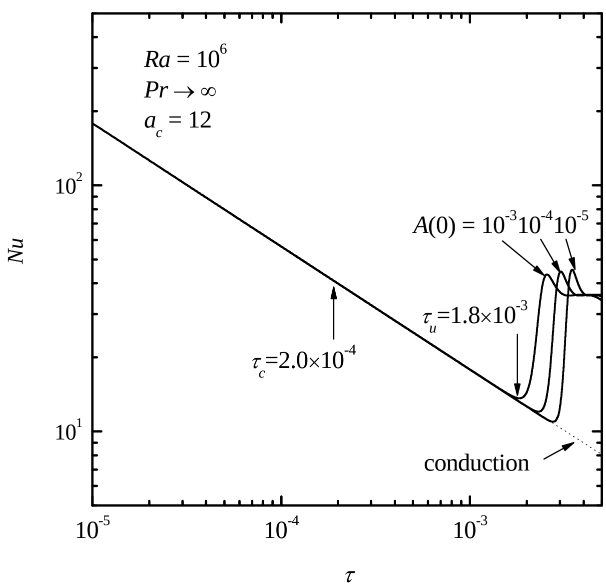

Fig. 5. Temporal behavior of Nusselt number

rigid upper boundary considering their rigid-boundary characteristics by replacing the boundary conditions (4a) with (5a). The onset time of convection for the fluid layer between two rigid boundaries cooled from above represents their experimental data to a certain degree. But this peculiar phenomenon for the gas absorption into wate require a futher justification.

6 Conclusion

For $Pr \to \infty$, the critical time to mark the onset of convective instability in the horizontal fluid layer cooled isothermally from above has been investigated by using the FVM. In the present study the characteristic times, τ_c and τ_u, have been predicted. We suggest that a fastest growing instability sets in at $\tau = \tau_c$ with $r_{1,\mathrm{T}} = r_{0,\mathrm{T}}$. Since τ_c is the invariant, which is independent of the initial magnitude of temperature fluctuations A(0) in the numerical simulation, it is here called the onset time of intrinsic instability.

With the assumed A(0)-value the undershoot time τ_u was obtained in comparison with the existing experimental data. The proper A(0)-value is found to be 10^{-3} in the present system. The manifest convection is surely observed at $\tau = \tau_u$. Since convective motion can be detected earlier at $\tau = \tau_D$ ($\le \tau_u$), we suggest the relation of $\tau_c \le \tau_D \le \tau_u$.

The present numerical simulation follows the actual phenomena reasonably well for $\tau_c \le \tau \le \tau_u$ and also clarifies the meaning of the characteristic times τ_c, τ_D and τ_u.

Acknowledgement

This work was supported by Grant Number R01-2004-000-10736-0 from the Basic Research Program of the Korea Science & Engineering Foundation.

References:

[1] B.R. Morton, On the Equilibrium of a Stratified Layer of Fluid, *Journal of Mechanical Applied Mathematics*, Vol. 10, 1957, pp 433-447.

[2] C.K. Choi, K.H. Kang, M.C. Kim, Convective Instabilities and Transport Properties in Horizontal Fluid Layers, *Korean Journal of Chemical Engneering*, Vol. 15, 1998, pp. 192-198.

[3] T.D. Foster, Stability of Homogeneous Fluid Cooled Uniformly from Above, *Physics of Fluids*, Vol. 8, 1965, pp. 1249-1257.

[4] B.S. Jhaveri, G.M. Homsy, The Onset of Convection in Fluid Layer Heated Rapidly in a Time-Dependent Manner, *Journal of Fluid Mechanics*, Vol. 114, 1982, pp. 251-260.

[5] K.K. Tan, R.B. Thorpe, The Onset of Convection Caused by Buoyancy during Transient Heat Conduction in Deep Fluids, *Chemical Engineering Science*, Vol. 51, 1996, pp. 4127-4136.

[6] W.G. Spangenberg, W.R. Rowland, Convective

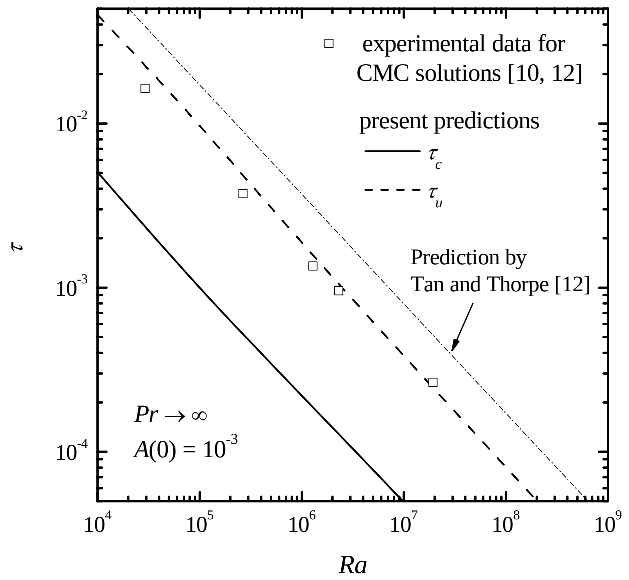

Fig. 6. Comparison of predictions with experiments

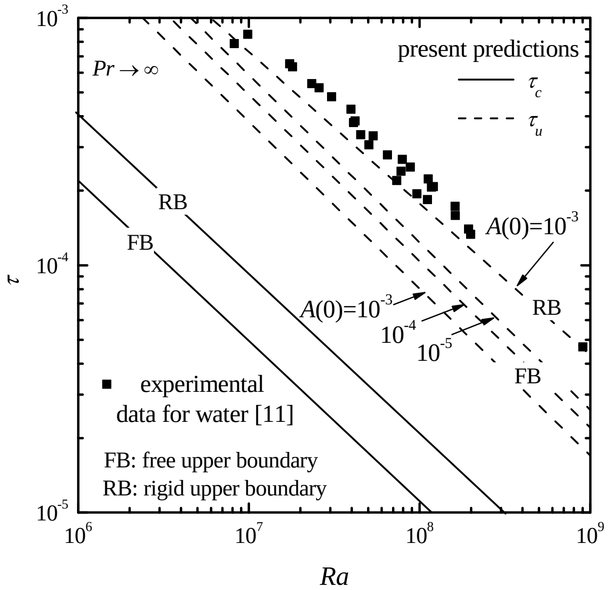

Fig. 7. Comparison with water experiments

Circulation in Water Induced by Evaporative Coooling, *Physics of Fluids*, Vol. 4, 1961, pp. 743-750.

[7] T.D. Foster, Onset of Convection in a Layer of Fluid Cooled from Above, *Physics of Fluids*, Vol. 8, 1965, pp. 1770-1774.

[8] M. Kaviany, The Onset of Thermal Convection in a Fluid Layer with Time-Dependent Temperature Distribution, *International Journal of Heat and Mass Transfer*, Vol. 27, 1984, pp. 375-380.

[9] C.K. Choi, J.H. Park, M.C. Kim, The Onset of Buoyancy-Driven Convection in a Horizontal Fluid Layer Subjected to Evaporative Cooling, *Heat and Mass Transfer*, Vol. 41, 2004, pp. 155-162.

[10] R.E. Plevan, J.A. Quinn, The Effect of Monomolecular Films on the Rate of Gas Absorption into a Quiescent Liquid, *AIChE Journal*, Vol. 12, 1965, pp. 894-902.

[11] L.M. Blair, J.A. Quinn, The Onset of Cellular Convection in a Fluid Layer with Time-Dependent Density Gradients, *Journal of Fluid Mechanics*, Vol. 36, 1969, pp. 385-400.

[12] K.K. Tan, R.B. Thorpe, Gas Diffusion into Viscous and Non-Newtonian Liquids, *Chemical Engineering Science*, Vol. 47, 1992, pp. 3565-3572.

[13] S.V. Patankar, *Numerical Heat Transfer and Fluid Flow*, Taylor & Francis, New York, 1980

[14] C.K. Choi, J.H. Park, H.K. Park, H.J. Cho, T.J. Chung and M.C. Kim, Temporal Evolution of Thermal Convection in an Initially Stably-Stratified Horizontal Fluid Layer, *International Journal of Thermal Sciences*, Vol. 43, 2004, pp. 817-823.

[15] T.J. Chung, M.C. Kim, C.K. Choi, The Temporal Evolution of Thermal Instability in Fluid Layers Isothermally Heated from Below, *Korean Journal of Chemical Engineering*, Vol. 21, 2004, pp. 41-47.

[16] T.D. Foster, Onset of Manifest Convection in a Layer of Fluid with a Time-Dependent Surface Temperature, *Physics of Fluids*, Vol. 12, 1969, pp. 2482-2487.

[17] K.K. Tan, R.B. Thorpe, The Onset of Convection Driven by Buoyancy Effects Caused by Various Modes of Transient Heat Conduction: Part I. Transient Rayleigh Numbers, *Chemical Engineering Science*, Vol. 54, 1999, pp. 225-238.